

X-Ray Resonance Exchange Scattering in UAs

E. D. Isaacs and D. B. McWhan

AT&T Bell Laboratories, 600 Mountain Avenue, Murray Hill, New Jersey 07974

C. Peters and G. E. Ice

Oak Ridge National Laboratory, Oak Ridge, Tennessee 37831

D. P. Siddons and J. B. Hastings

Brookhaven National Laboratory, Upton, New York 11973

C. Vettier

Institut Laue-Langevin, 38052 Grenoble CEDEX, France

O. Vogt

Eidgenössische Technische Hochschule Zürich-Hönggerberg, Zürich, Switzerland

(Received 29 December 1988)

Resonant enhancement of the magnetic x-ray scattering cross section in UAs has been investigated by tuning the incident x-ray energy through the uranium M_{IV} and M_V absorption edges. At the M_{IV} edge the intensity for the $(0,0,\frac{1}{2})$ magnetic reflection is enhanced by 10^7 relative to the nonresonant component far above the edge, and is a remarkable 1% of the intensity at the $(0,0,2)$ charge peak. At the M_V edge the enhancement is 10^5 . The dramatic enhancement at M edges has been predicted by Hannon *et al.*, and arises from strong electric multipole transitions between atomic core states and the exchange-split Fermi-edge states.

PACS numbers: 78.70.Ck, 61.10.-i

In recent experimental work Gibbs *et al.*¹ demonstrated a fiftyfold enhancement of the magnetic scattering cross section when the incident x-ray energy was tuned through the L_{III} ($2p_{3/2}$ to $5d$, 8.067 keV) absorption edge of holmium. Guided by the energy and polarization dependence of these results, Hannon *et al.* explained the observed enhancement through strong electric multipole transitions from atomic core states to the unoccupied Fermi-edge states.² Sensitivity to the magnetization arises from the Pauli exclusion principle and the exchange-induced splitting of the Fermi-edge states. A much larger enhancement was predicted at the M_{IV} and M_V edges since the dipole transitions are to narrow $4f$ states in contrast to the more extended $5d$ band states at the L_{III} edge. In this paper we demonstrate the enhancement of the magnetic scattering cross section at the M edge of uranium in the antiferromagnet UAs. At the peak of the resonance for the M_{IV} edge ($3d_{3/2}$ to $5f_{5/2}$, 3.728 keV) the scattering intensity at the $(0,0,\frac{1}{2})$ magnetic reflection is 1% of the intensity at the $(0,0,2)$ reflection. This represents a resonant enhancement of 7 orders of magnitude in the magnetic scattering. The polarization dependence at the M_{IV} edge is in agreement with the polarization selection rules for the appropriate atomic dipole transition. The enhancement at the M_V edge ($3d_{5/2}$ to $5f$, 3.552 keV) for the same magnetic reflection is 10^5 .

UAs has the NaCl crystal structure, and the magnetic structure is well known from neutron scattering data.³⁻⁵ At $T=127$ K the uranium moments order as a type-1

antiferromagnet with a magnetic moment of approximately 2 Bohr magnetons per uranium atom. At $T=63$ K, UAs exhibits a first-order phase transition into a type-1A $2-q$ structure. For the $2-q$ structure the Fourier components of the magnetization are $(\frac{1}{2},0,0)$ and $(0,\frac{1}{2},0)$ with the net moment lying along the $[110]$. There are three possible magnetic domains associated with this structure and each domain gives rise to two sets of magnetic Bragg peaks. For example, the domain labeled (xy) results in the $(0,\pm\frac{1}{2},2)$ and $(\pm\frac{1}{2},0,2)$ satellite peaks about the $(0,0,2)$ charge peak, while the (yz) domain gives rise to the $(0,\pm\frac{1}{2},2)$ and $(0,0,2\pm\frac{1}{2})$ satellite peaks. Thus, each of the magnetic Bragg peaks is the sum of contributions from two of the domains. In the absence of strain the three domains are equally populated.³

The total coherent elastic x-ray scattering amplitude is given by $f=f_0+f'+if''+f_{\text{mag}}$, where f_0 is the Fourier transform of the charge density. f_{mag} is the nonresonant magnetic amplitude and is of the form $\mathbf{L}(\mathbf{K})\cdot\mathbf{A}+\mathbf{S}(\mathbf{K})\cdot\mathbf{B}$. $\mathbf{L}(\mathbf{K})$ and $\mathbf{S}(\mathbf{K})$ are the Fourier transforms of the orbital momentum and spin densities, respectively, and \mathbf{A} and \mathbf{B} are polarization vectors given by the geometry of the experiment.^{6,7} Nonresonant magnetic x-ray scattering is described in detail elsewhere.^{1,6-11} Resonant magnetic scattering, which is a special case of anomalous scattering, arises from dispersive and absorptive phenomena, represented by the terms $f'+if''$. In this two-photon, coherent, elastic process the intermediate state is a localized exciton, which decays via radiative

recombination to the original ground state of the atom. Sensitivity to the magnetization arises from the Pauli exclusion principle, allowing optical transitions only to unoccupied states, and the exchange splitting of the Fermi-edge states.

The scattering amplitude which gives rise to coherent, first-order antiferromagnetic scattering in UAs is given by²

$$f^{\text{res}}(\omega, \hat{\epsilon}_i, \hat{\epsilon}_f) = -i \frac{3}{4} \lambda (\hat{\epsilon}_f^* \times \hat{\epsilon}) \cdot \hat{\mathbf{z}}_j [F_{11}(\omega) - F_{1-1}(\omega)], \quad (1)$$

where $\lambda = \lambda/2\pi$, $\hat{\epsilon}_i$ and $\hat{\epsilon}_f$ are the electric polarization vectors for the incident and scattered x rays, respectively, and $\hat{\mathbf{z}}_j = \mathbf{M}(\mathbf{r})/M$ is a unit vector in the direction of the magnetization. The $F_{lm}(\omega)$'s are a function of the incident x-ray energy only and not its polarization. Their magnitude depends on overlap integrals between the atomic ground state and the intermediate excitonic states, a resonant denominator, and the fluorescence yield. These highly localized excitonic states, which can be treated as "impurity" exchange-split Fermi-edge states in the presence of a core hole, give rise to large enhancements in the density of states just below the absorption edge. This enhancement, observed as the "white line" in absorption and electron emission spectra, can be very large at absorption edges where the Fermi-edge states are either atomic orbitals or narrow bands.¹² Such is the case, for example, at the M_{IV} and M_V edges in uranium, which correspond to transitions from the core $3d_{3/2}$ and $3d_{5/2}$, respectively, to an exciton formed from the narrow $5f_{5/2}$ and $5f_{7/2}$ band and the $3d$ hole. On the other hand, a considerably weaker enhancement is expected for the M_{III} edge in uranium, where a $3p_{3/2}$ core state couples via a dipole transition to a $6d$ band and via quadrupole transitions to the $5f$ band. The M_{III} edge is similar to the L_{III} edge in holmium where the hole state is $2p_{3/2}$ rather than $3p_{3/2}$. Previous experiments at the L_{III} edge of holmium showed a resonant enhancement of 50.¹

The experiments were carried out at the Oak Ridge National Laboratory beam line X14 at the National Synchrotron Light Source (NSLS), Brookhaven National Laboratory.¹² This line incorporates sagittal crystal focusing to condense 5 mrad of synchrotron radiation with a tunable range of 2.5 to 40 keV. The fixed-exit, double-crystal, Si(111) monochromator has an energy resolution of better than 1 eV from 2.5 to 6 keV. Of particular concern for this experiment was the presence of harmonics passed by the monochromator, mainly $\lambda/3$ and $\lambda/4$. Charge scattering of these higher harmonics was in some cases superimposed over the magnetic scattering. Harmonic contamination was reduced by several orders of magnitude by detuning the monochromator to half the peak intensity. Further reduction in the harmonic contamination was achieved by using a neon-carbon-dioxide-filled proportional counter as the

detector. The sensitivity of the neon-carbon-dioxide gas varies as $1 - \exp[-\text{const} \times \lambda^3]$. In addition, the energy resolution of the neon detector was sufficient to discriminate between the fundamental and the harmonic scattering with a multichannel analyzer. The detector was calibrated relative to an Fe⁵⁵ source. The estimated uncertainty in the absolute energy of the incident beam was less than 10 eV.

In order to compare Eq. (1) with experiment, the polarization of the incident and scattered beams must be known. Following the convention of Refs. 1, 2, and 7 the components of linear polarization are defined as σ and π . The σ component is perpendicular to the scattering plane, which is spanned by \mathbf{k}_i and \mathbf{k}_f . The π component is in the scattering plane and normal to either \mathbf{k}_i or \mathbf{k}_f , respectively. The linear components of polarization were measured with an aluminum analyzer crystal. When the incident photon energy is tuned to 3.75 keV the Bragg angle for the Al(111) reflection is 45°. Thus, only the polarization vector normal to the Al scattering vector is reflected into the detector. Upon rotation of the Al crystal by 90° about the axis of the beam scattered from the sample, the other component of polarization is detected. At the energy of the M_{IV} edge of uranium there is a small change in the Bragg angle to 45.4°. This results in a small amount of crosstalk between the two polarizations of the scattered beam. The polarization of the incident beam was found to be 85% σ polarized when integrated over the rocking curve of the Al(111) analyzer crystal.

A single [001] plate of UAs was mounted on the cold finger of a closed-cycle ⁴He refrigerator which was equipped with a cylindrical beryllium cap. The refrigerator was mounted at the center of a large four-circle diffractometer so as to give a $(0kl)$ scattering plane at $\chi = 0$. In order to minimize the absorption of the 3-5-keV x rays the entire flight path was either under vacuum or slightly overpressured with He gas. In addition, no heat shields were used. Note that at 3.5 keV the absorption coefficient for nitrogen is 10 cm⁻¹ and a 10-mil beryllium window absorbs half of the incident photons.

In order to obtain accurate relative scattering intensities for the different reflections, the beam size was reduced, with tantalum slits, to be slightly smaller than the sample area at the smallest scattering angle [i.e., at the $(0, 0, \frac{3}{2})$ reflection]. Slits were only required in the vertical since the horizontal focus was considerably smaller than the sample. The beam intensity was monitored after the slits with a helium-filled ionization chamber (99.999% purity).

The transition from the type-1 to type-1A structure in UAs corresponds to a doubling of the magnetic unit cell. This is illustrated in the inset of Fig. 1. At the transition temperature the intensity of the $(0, 0, 1)$ magnetic reflection vanishes, while the intensity of the $(0, \frac{1}{2}, 2)$ magnetic reflection has a sharp onset. The apparent 3-K

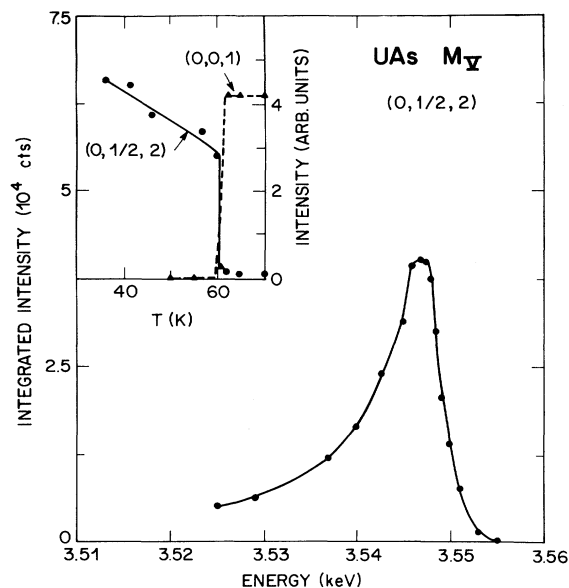


FIG. 1. Total integrated intensity vs incident x-ray energy at the M_V absorption edge of uranium. Inset: Temperature dependence of the reflections from the type-1 $(0,0,1)$ and type-1A $(0, \frac{1}{2}, 2)$ structures.

discrepancy in the transition temperature from previous studies probably resulted from the absence of heat shields around the sample and the fact that the GaAs diode sensor was mounted about 0.5 cm below the sample.

The energy dependence of the integrated intensity (no polarization analyzer) for the $(0, \frac{1}{2}, 2)$ magnetic reflection through the M_V absorption edge of uranium is shown in Fig. 1. At the peak of the resonance curve the magnetic scattering intensity is $\sim 0.01\%$ of the intensity at the $(0,0,2)$ charge peak or 10^5 times larger than the expected nonresonant magnetic scattering intensity. The resonance line shape shows a long, asymmetric low-energy tail and peaks slightly below the edge. The linewidth, which arises from the excitonic lifetime at the absorption edge, is approximately 10 eV FWHM. In a flat-plate geometry the measured intensity is multiplied by the absorption factor to obtain the scattering cross section. For many uranium compounds there is a large change in the absorption at the edge and an associated white line (see, for example, Ref. 13). No measurements of the absorption coefficient in UAs have been reported in the literature and consequently, the data have not been corrected for absorption. This correction would tend to emphasize the peak height and to a smaller degree the high-energy side of the resonance. The M_V -edge line shape is similar to the L_{III} edge of holmium for σ to π polarization. The asymmetry of the line shape in the holmium was attributed to the coherent sum of the resonant dipole and nonresonant magnetic scattering with different phases.² However, in UAs, at the M_V edge

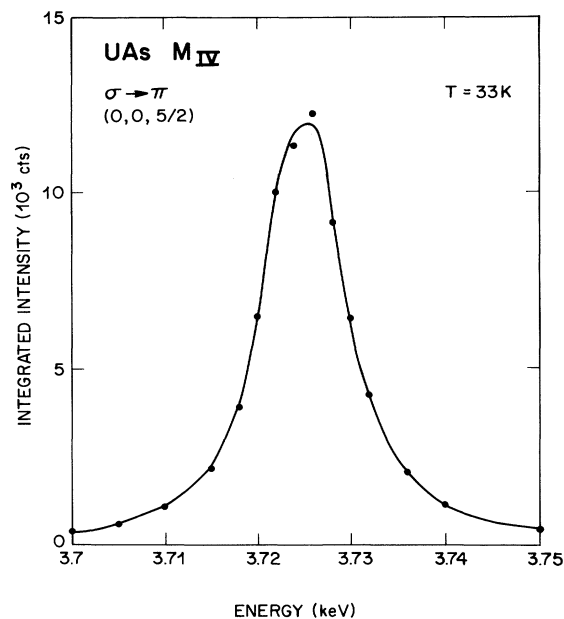


FIG. 2. Integrated intensity for the component of polarization which is rotated upon scattering vs energy at the M_V absorption edge of uranium.

the relative amplitude of the nonresonant term is so small that the interference effects should be too weak to observe. Our preliminary measurements of the intensity in the tails suggest that the asymmetry of the M_V -resonance line shape arises from interference with the low-energy tail of the M_{IV} resonance.

Figure 2 shows the energy dependence of the integrated intensity for the σ to π polarization of the $(0,0, \frac{5}{2})$ magnetic reflection through the M_{IV} absorption edge of uranium. At the peak of the resonance the scattering intensity was 0.76% of the intensity at the $(0,0,2)$ (σ to σ polarization). This corresponds to a resonant enhancement of the magnetic scattering cross section of a factor of 8×10^6 or an absolute scattering amplitude of $9r_0$. The intensity for the σ to σ polarization of the $(0,0, \frac{5}{2})$ was 2 orders of magnitude weaker at the peak of the resonance. This amount of σ to σ scattering is consistent with Eq. (1) when we consider the incomplete polarization of the incident beam, which leads to π to σ scattering, and a polarization analyzer efficiency that was less than 100%, allowing σ to π scattering to be passed.

In holmium, which has a spiral antiferromagnetic structure, theory and experiment have shown that for a dipole resonance magnetic scattering should occur at both the first and the second harmonic.^{1,2} The second harmonic arises from a quadratic contribution to the scattering amplitude proportional to $(\hat{\epsilon}_f \cdot \hat{z}_j)(\hat{\epsilon}_i \cdot \hat{z}_j)$. However, this contribution is invariant under inversion, $\hat{z}_j \rightarrow -\hat{z}_j$, so there should be no second harmonic for the type-1A structure of UAs which has a $(+ + - -)$ antiferromagnetic superlattice. First and second har-

TABLE I. Relative intensities of the six magnetic satellite reflections compared with Eq. (1). The observed ratios are corrected for relative absorption and are normalized to the $(0,0,\frac{5}{2})$ reflection. The calculated values assume equal populations for each of the three domains and pure σ polarization.

h	k	l	Observed	Calculated
0	0	$\frac{5}{2}$	1	1
0	0	$\frac{3}{2}$	0.6	0.68
0	$\frac{1}{2}$	2	1.17	1.51
0	$-\frac{1}{2}$	2	0.78	1.22
$\frac{1}{2}$	0	2	0.071	0.045
$-\frac{1}{2}$	0	2	0.049	0.045

monics would correspond to reflections at, for example, $(0,0,2 \pm \frac{1}{2})$ and $(0,0,2 \pm 1)$. The measurements shown in the inset of Fig. 1 set an upper limit on the ratio of the intensity of the second to the first harmonic of $I(0,0,1)/I(0,0,\frac{5}{2}) < 0.01$. The limit is set by possible charge scattering from magnetoelastic distortion and the contamination from the $\lambda/2$ $(0,0,2)$ and $\lambda/4$ $(0,0,4)$ charge peaks.

The total integrated scattering intensities at the six magnetic satellites around the $(0,0,2)$ were measured at the peak of the M_{IV} resonance. The results are compared with those calculated from Eq. (1) in Table I. The calculated intensities were normalized to the $(0,0,\frac{5}{2})$ reflection and corrected for variations in the Lorentz factor and for the difference in x-ray path, and hence absorption, when the angle of incidence was not equal to the angle of reflection. The correction factor is $\frac{1}{2} [1 + \sin(\theta + \omega)/\sin(\theta - \omega)]$, where θ is the Bragg angle and $\omega = \pm \arctan(k/l)$. Finally, a correction was made for the angular variation of the absorption of the incident and scattered beams by the beryllium cap in the cryostat. The calculated values assume that each of the three magnetic domains are equally populated (see Ref. 3) and that the polarization of the incident photon is pure σ . The agreement between the theory and experiment is additional support for attributing the magnetic scattering enhancement to electric dipole transitions.

We have demonstrated resonant enhancements of the magnetic scattering cross section as large as 10^7 at the

M_{IV} and M_V edges of uranium in UAs. The magnitude and polarization of the data are in qualitative agreement with the theory of Hannon *et al.*² Larger enhancements are expected at the lower-energy rare-earth M edges. Although it is technically more challenging to carry out diffraction studies at soft-x-ray edges, it may be possible to study, for example, surface magnetism in the rare-earth metals like holmium.

We thank J. D. Axe, M. Blume, Doon Gibbs, J. P. Hannon, P. M. Platzman, M. Schlutter, G. T. Trammell, C. Varma, and J. Zegenhagen for helpful discussions. NSLS is supported by the U.S. Department of Energy under Contract No. DE-ACO2-76CH0016 and Oak Ridge National Laboratory under Contract No. DE-ACO5-84OR21400 with the Martin Marietta Energy Systems, Inc.

¹Doon Gibbs, D. R. Harshman, E. D. Isaacs, D. B. McWhan, D. Mills, and C. Vettier, Phys. Rev. Lett. **61**, 1241 (1988).

²J. P. Hannon, G. T. Trammell, M. Blume, and Doon Gibbs, Phys. Rev. Lett. **61**, 1245 (1988).

³J. Rossat-Mignod, P. Burlet, H. Bartholin, R. Tchapoutian, O. Vogt, C. Vettier, and R. Langier, Physica (Amsterdam) **102B**, 177 (1980).

⁴S. K. Sinha, G. H. Lander, S. M. Shapiro, and O. Vogt, Physica (Amsterdam) **102B**, 174 (1980).

⁵M. Kuznietz, P. Burlet, and J. Rossat-Mignod, J. Magn. Magn. Mater. **69**, 12 (1987).

⁶M. Blume, J. Appl. Phys. **57**, 3615 (1985).

⁷M. Blume and Doon Gibbs, Phys. Rev. B **37**, 1779 (1988).

⁸P. M. Platzman and N. Tzoar, Phys. Rev. B **2**, 3556 (1970).

⁹F. DeBergevin and M. Brunel, Acta Crystallogr. Sect. A **37**, 314 (1981).

¹⁰O. L. Zhizhimov and I. B. Khriplovich, Zh. Eksp. Teor. Fiz. **87**, 547 (1984) [Sov. Phys. JETP **60**, 313 (1984)].

¹¹S. Lovesey, J. Phys. C **20**, 5625 (1987).

¹²A. Habenschuss, G. E. Ice, C. J. Sparks, and R. A. Neiser, Nucl. Instrum. Methods Phys. Res., Sect. A **266**, 215 (1988).

¹³E. E. Alp, G. K. Shenoy, L. Soderholm, D. G. Hinks, J. Guo, and D. E. Ellis, National Synchrotron Light Source Annual Report, 1987 (unpublished), p. 3-69; G. Kalkowski, G. Kaindl, W. D. Brewer, and W. Krone, Phys. Rev. B **35**, 2667 (1987).